A New Methodology for Tolerance Synthesis of Parallel Manipulators

Alexandre Goldsztejn, Gilles Chabert, Stéphane Caro

The 14th IFToMM World Congress, Taipei, Taiwan, October 25-30, 2015
DOI Number: 10.6567/IFToMM.14TH.WC.OS12.017

A New Methodology for Tolerance Synthesis of Parallel Manipulators

A. Goldsztejn* S. Caro† G. Chabert‡
IRRCyN, CNRS IRCCyN, CNRS LINA, Ecole des Mines de Nantes
Nantes, France Nantes, France Nantes, France

Abstract— *Computing the maximal pose error given an upper bound on perturbations is challenging for parallel robots, mainly because the direct kinematic problem has several solutions, which become unstable near or at parallel singularities. In this paper, we propose a local uniqueness hypothesis that will allow safely computing pose error upper bounds using nonlinear optimization. This hypothesis, together with a corresponding maximal allowed perturbation domain and a certified pose error upper bound valid over the complete workspace, will be proved numerically using a parametric version of Kantorovich theorem and certified nonlinear global optimization. We will then show how to synthesize tolerances reaching a prescribed maximal pose error over a workspace using approximate linearizations. This approximate tolerance synthesis will finally be checked using the certified pose error upper bound we propose. Preliminary experiments on a RPRPR and a 3RPR with fixed orientation parallel manipulators are presented.*

Keywords: Certified tolerance synthesis, parallel manipulators, Kantorovich Theorem

I. Introduction

For two decades, parallel manipulators have attracted the attention of more and more researchers who consider them as valuable alternative design for robotic mechanisms. As stated by some authors, conventional serial kinematic machines have already reached their dynamic performance limits, which are bounded by high stiffness of the machine components required to support sequential joints, links and actuators. Thus, while having good operating characteristics (large workspace, high flexibility and maneuverability), serial manipulators have disadvantages of low stiffness and low power. Conversely, Parallel Kinematics Machines (PKM) offer essential advantages over their serial counterparts (lower moving masses, higher stiffness and payload-to-weight ratio, higher natural frequencies, better accuracy, simpler modular mechanical construction, possibility to locate actuators on the fixed base).

However, PKM are not necessarily more accurate than their serial counterparts. Indeed, even if the dimensional variations can be compensated with PKM, they can also be amplified contrary to with their serial counterparts. Wang et al. [19] studied the effect of manufacturing tolerances on the accuracy of a Stewart platform. Kim et al. [12] used a forward error bound analysis to find the error bound of the end-effector of a Stewart platform when the error bounds of the joints are given, and an inverse error bound analysis to determine those of the joints for the given error bound of the end-effector. Kim and Tsai [13] studied the effect of misalignment of linear actuators of a 3-DOF translational parallel manipulator on the motion of its moving platform. Han et al. [11] used a kinematic sensitivity analysis method to explain the gross motions of a 3-UPU parallel mechanism, and showed that it is highly sensitive to certain minute clearances. Fan et al. [9] analyzed the sensitivity of the 3-PRS parallel kinematic spindle platform of a serial-parallel machine tool. Verner et al. [18] presented a new method for optimal calibration of PKM based on the exploitation of the least error sensitive regions in their workspace and geometric parameters space. As a matter of fact, they used a Monte Carlo simulation to determine and map the sensitivities to geometric parameters. Moreover, Caro et al. [4] developed a tolerance synthesis method for mechanisms based on a robust design approach.

During the early design process of engineering systems, the analysis of the performance sensitivity to uncertainties is an important task. High sensitivity to parameters that are inherently noisy can lead to poor, or unexpected performance. For that reason, it is important to analyze the sensitivity of their performance to variations in their geometric parameters and to determine the optimal dimensional tolerances.

To this end, some indices such as the dexterity and the manipulability have been used to evaluate the sensitivity of robots performance to variations in their actuated joints [20], [2], [14]. However, they are not suitable for the evaluation of this sensitivity to other types of uncertainty such as variations in geometric parameters. Two indices were proposed in [6] to evaluate the sensitivity of the end-effector pose (position + orientation) of the Orthoglide 3-axis, a three Degree-of-Freedom (DOF) translational PKM, to variations in its design parameters. In the same vein, four 3-RPR planar parallel manipulators (PPMs) were compared in [5] based on the sensitivity of their performance to variations in their geometric parameters. In [16], an interval linearization method is used for the sensitivity analysis of some parallel manipulators. However, the foregoing research works do not deal with the tolerance synthesis of

*Alexandre.Goldsztejn@irccyn.ec-nantes.fr
†Stephane.Caro@irccyn.ec-nantes.fr
‡Gilles.Chabert@mines-nantes.fr

parallel manipulators, which is a critical issue.

In the present paper, we overcome two lacks in the literature: First, a fully rigorous methodology is proposed to compute a certified upper bound for the pose error due to perturbations of the parameters of a PKM over a full workspace. Second, a methodology is proposed for tolerance synthesis of PKM, aiming synthesizing the largest tolerances keeping the pose error below a given limit.

The paper is organized as follows: In Section III, we first introduce a uniqueness hypothesis that allows computing a certified pose error upper bound over a given workspace by solving a nonlinear optimization problem. Second, we propose a parametric version of Kantorovich theorem, which provides both a maximal perturbation domain for which this uniqueness hypothesis holds, and a crude certified pose error upper bound valid inside this perturbation domain and the whole workspace. As a result, for perturbations within this maximal perturbation domain, some sharp pose error upper bounds can be computed using the nonlinear optimization problem previously introduced. In Section IV, we propose an approximate linearization of the maximal error in the workspace, which allows performing some approximate tolerance synthesis. These approximate tolerances can finally be corrected using the results of Section III. Preliminary experiments on a RPRPR and a 3RPR with fixed orientation parallel manipulators are presented in Section V, which show the potential and the limits of the approach.

Notations

We use the ∞-norm throughout the paper. Let $B(\mathbf{x},\epsilon)$ be the open ball $\{\mathbf{y}\in\mathbb{R}^k : \|\mathbf{y}-\mathbf{x}\|<\epsilon\}$, $\overline{B}(\mathbf{x},\epsilon)$ be the closed ball $\{\mathbf{y}\in\mathbb{R}^k : \|\mathbf{y}-\mathbf{x}\|\leq\epsilon\}$, and for short $\overline{B}_\epsilon := \overline{B}(\mathbf{0},\epsilon)$.

II. Basic notations and definitions

We consider a kinematic model $\mathbf{f}(\mathbf{x},\mathbf{q},\mathbf{p})$ of a non-redundant parallel manipulator, where $\mathbf{f} : \mathbb{R}^n \times \mathbb{R}^n \times \mathbb{R}^m \to \mathbb{R}^n$, $\mathbf{x}$ being the pose, $\mathbf{q}$ the actuated joint coordinates and $\mathbf{p}$ a perturbation vector, so that the nominal model is $\mathbf{f}(\mathbf{x},\mathbf{q},\mathbf{0})$. We also denote this nominal model by $\mathbf{f}(\mathbf{x},\mathbf{q}) := \mathbf{f}(\mathbf{x},\mathbf{q},\mathbf{0})$. We suppose that $\mathbf{f}$ is differentiable and has locally Lipschitz continuous first derivatives with respect to pose and perturbation, e.g., $\mathbf{f}$ is twice differentiable with respect to these variables. The Jacobian matrix of $\mathbf{f}$ with respect to variables $\mathbf{x}$ and $\mathbf{p}$ are denoted respectively as $\mathbf{F}_\mathbf{x}$, called the kinematic parallel Jacobian matrix, and $\mathbf{F}_\mathbf{p}$, called the sensitivity Jacobian matrix.

The nominal generalized workspace is defined by

$$\mathcal{G} := \{(\mathbf{x},\mathbf{q})\in\mathbb{R}^{2n} : \mathbf{f}(\mathbf{x},\mathbf{q})=\mathbf{0}, \mathbf{g}(\mathbf{x},\mathbf{q})\leq\mathbf{0}\}, \quad (1)$$

where $\mathbf{g}$ is a set of inequalities that defines the generalized workspace of interest. We assume that $\mathcal{G}$ is bounded. We also require that $\mathcal{G}$ does not contain any parallel singularity, but this will be checked by the proposed method.

In some situations, the kinematic model can be solved for the pose coordinates inside $\mathcal{G}$, giving rise to a direct model $\mathbf{d} : \mathbb{R}^n \to \mathbb{R}^n$ that provides an explicit description of the nominal generalized workspace:

$$\mathbf{x}=\mathbf{d}(\mathbf{q}) \wedge g(\mathbf{x},\mathbf{q})\leq 0 \iff (\mathbf{x},\mathbf{q})\in\mathcal{G}. \quad (2)$$

When perturbations are to be taken into account, we expect to have a direct model that depends of perturbations: $\mathbf{x}=\mathbf{d}(\mathbf{q},\mathbf{p})$. Such a direct model cannot be correct for arbitrarily large perturbations, and therefore has to be associated to a perturbation domain $\mathcal{P}$ for which it is valid (for simplicity, the perturbation domain $\mathcal{P}$ is supposed to contain $\mathbf{0}$ and to be convex). Although such a direct model with explicit dependence on perturbations naturally arises in the context of serial robots, it is usually quite difficult to obtain for parallel robots.

III. Upper bounds for maximal pose errors

In this section, we compute an upper bound on the distance between a nominal pose and its perturbed pose. In the first subsection, we introduce an uniqueness condition that allows associating the nominal and perturbed posed unambiguously, which is obviously required to compute the distance between them. In the second subsection, we show how Kantorovich theorem can be used in a parametric way within the whole generalized workspace and perturbation space in order to provide both a perturbation domain for which the above uniqueness condition holds, and a pose error upper bound valid within the whole workspace and for all considered perturbations.

A. General framework

When an explicit direct model $\mathbf{x}=\mathbf{d}(\mathbf{q},\mathbf{p})$ is available, finding the maximal pose error over the workspace can be modeled by the following constrained optimization problem:

$$\max_{\substack{(\mathbf{x},\mathbf{q})\in\mathcal{G},\mathbf{p}\in\mathcal{P}\\ \mathbf{x}'=\mathbf{d}(\mathbf{q},\mathbf{p})}} e(\mathbf{x},\mathbf{x}'), \quad (3)$$

see e.g. [3]. The variables are the joint coordinates $\mathbf{q}\in\mathbb{R}^n$, the nominal pose $\mathbf{x}\in\mathbb{R}^n$, the perturbed pose $\mathbf{x}'\in\mathbb{R}^n$ and the perturbation $\mathbf{p}\in\mathbb{R}^m$. The constraint $(\mathbf{x},\mathbf{q})\in\mathcal{G}$ states that $(\mathbf{x},\mathbf{q})$ is a nominal configuration, while the constraint $\mathbf{x}'=\mathbf{d}(\mathbf{q},\mathbf{p})$ states that $\mathbf{x}'$ is the perturbed pose corresponding to the same joint coordinates $\mathbf{q}$. The cost function $e(\mathbf{x},\mathbf{x}')$ is an error measurement (we consider here either the norm of the positioning error or the norm of the orientation error, so $e(\mathbf{x},\mathbf{x}')=\|\mathbf{\Pi}(\mathbf{x}-\mathbf{x}')\|$ where $\mathbf{\Pi}$ is a projection on a subset of the coordinates of the pose).

The aim of this section is to generalize this approach to the case where the direct model with explicit dependence on perturbations is not available. The naive generalization

$$\max_{\substack{(\mathbf{x},\mathbf{q})\in\mathcal{G},\ \mathbf{p}\in\mathcal{P}\\ \mathbf{f}(\mathbf{x}',\mathbf{q},\mathbf{p})=\mathbf{0}}} e(\mathbf{x},\mathbf{x}') \quad (4)$$

is not correct because the direct kinematic problem may have several solutions or no solution at all for a given perturbation. This means that the maximum of $e(\mathbf{x}, \mathbf{x}')$, if defined, is likely to be reached for a $\mathbf{x}'$ that does not corresponds to a perturbation of $\mathbf{x}$, i.e., the optimization problem (4) makes no sense. Hence, the perturbation domain has to be small enough so that perturbing the nominal pose leads to a solution and a unique one.

We formalize this restriction as follows: For given $\overline{\epsilon} > 0$, $\mathcal{G} \subseteq \mathbb{R}^n \times \mathbb{R}^n$ and $\mathcal{P} \subseteq \mathbb{R}^m$, we say that $\mathcal{G}$ is $\overline{\epsilon}$-*safe with respect to* $\mathcal{P}$ if

$$\forall (\mathbf{x}, \mathbf{q}) \in \mathcal{G}, \forall \mathbf{p} \in \mathcal{P}, \quad \exists! \, \mathbf{x}' \in \overline{B}(\mathbf{x}, \overline{\epsilon}), \mathbf{f}(\mathbf{x}', \mathbf{q}, \mathbf{p}) = \mathbf{0}. \quad (5)$$

The existence of a *unique* perturbed pose within $\overline{B}(\mathbf{x}, \overline{\epsilon})$ is crucial in this definition since it enforces a functional dependence between $\mathbf{x}'$ and $\mathbf{p} \in \mathcal{P}$, which we denote by $\mathbf{x}' = \mathbf{d}_{\mathbf{x},\mathbf{q}}(\mathbf{p})$. It is easy to check that this function is continuous, and that $\mathbf{d}_{\mathbf{x},\mathbf{q}}(\mathbf{0}) = \mathbf{x}$, which makes $\mathbf{x}' = \mathbf{d}_{\mathbf{x},\mathbf{q}}(\mathbf{p})$ the perturbed pose associated to the nominal pose $\mathbf{x}$ with no ambiguity. Therefore, under the hypothesis that $\mathcal{G}$ is $\overline{\epsilon}$-safe with respect to $\mathcal{P}$, we can safely use the kinematic model $\mathbf{f}(\mathbf{x}', \mathbf{q}, \mathbf{p}) = \mathbf{0}$ in order to characterize the perturbed pose:

$$\begin{array}{c} (\mathbf{x}, \mathbf{q}) \in \mathcal{G}, \mathbf{p} \in \mathcal{P} \\ \mathbf{x}' \in \overline{B}(\mathbf{x}, \overline{\epsilon}) \\ \mathbf{f}(\mathbf{x}', \mathbf{q}, \mathbf{p}) = \mathbf{0} \end{array} \iff \begin{array}{c} (\mathbf{x}, \mathbf{q}) \in \mathcal{G}, \mathbf{p} \in \mathcal{P} \\ \mathbf{x}' = \mathbf{d}_{\mathbf{x},\mathbf{q}}(\mathbf{p}) \end{array} . \quad (6)$$

As a consequence, even though no explicit expression of $\mathbf{d}_{\mathbf{x},\mathbf{q}}$ is available, the maximal error inside the nominal workspace is given by

$$\max_{\substack{(\mathbf{x},\mathbf{q}) \in \mathcal{G}, \, \mathbf{p} \in \mathcal{P} \\ \mathbf{x}' \in \overline{B}(\mathbf{x}, \overline{\epsilon}) \\ \mathbf{f}(\mathbf{x}', \mathbf{q}, \mathbf{p}) = \mathbf{0}}} e(\mathbf{x}, \mathbf{x}'). \quad (7)$$

As a conclusion, the constrained optimization problem (7) allows computing a sharp pose error upper bound, provided that the nominal generalized workspace $\mathcal{G}$ is proved to be $\overline{\epsilon}$-safe with respect to $\mathcal{P}$. The next subsection deals with the determination of $\mathcal{P}$ and $\overline{\epsilon}$ using Kantorovich theorem.

Remark 1: The error function in (7) can be chosen to be either the norm of the position error or the norm of the orientation error, which is interseting since aggregating these errors is often difficult or irrelevant. However, they have to be aggregated in the norm condition $\mathbf{x}' \in \overline{B}(\mathbf{x}, \overline{\epsilon})$ of (5), (6) and (7). The impact of this aggregation is on the size of the perturbation domain $\mathcal{P}$ (as it will be shown in the next section).

B. Parametric Kantorovich Theorem for $\overline{\epsilon}$-safety

B.1 Informal presentation

Kantorovich theorem [15], [10], [14], [8] is now applied in order to both provide a perturbation domain $\mathcal{P}$ and an error upper bound $\overline{\epsilon}$ for which $\mathcal{G}$ is $\overline{\epsilon}$-safe with respect to $\mathcal{P}$.

The basic idea is, for an arbitrary configuration $(\mathbf{x}, \mathbf{q}) \in \mathcal{G}$ and an arbitrary perturbation $\mathbf{p} \in \mathcal{P}$, to apply Kantorovich theorem for solving the perturbed direct kinematic problem $\mathbf{f}(\,\cdot\,, \mathbf{q}, \mathbf{p}) = 0$, with the nominal pose $\mathbf{x}$ as an initial condition. The perturbation domain $\mathcal{P}$ is going to be defined so that the hypotheses of Kantorovich Theorem are satisfied for every perturbation it contains. As a consequence, the existence and uniqueness regions provided by Kantorovich theorem are going to enforce $\mathcal{G}$ to be $\overline{\epsilon}$-safe with respect to $\mathcal{P}$, for a given $\overline{\epsilon}$ also provided by Kantorovich theorem.

The key feature of Kantorovich Theorem that allows applying it over the whole generalized workspace and perturbation space is that when the constants involved in Kantorovich Theorem are sharper, the size of the existence ball decreases and the size of the uniqueness ball increases. Therefore, worst case constants over $\mathcal{G}$ and $\mathcal{P}$ will provide a greatest existence domain and a smallest uniqueness domain valid over both $\mathcal{G}$ and $\mathcal{P}$.

B.2 The main theorem

Choose an apriori maximal tolerance $\overline{\Delta} > 0$ so that only perturbations satisfying $\|\mathbf{p}\| \in \overline{B}_{\overline{\Delta}}$ will be considered[1]. Then define the constants κ, χ and $\gamma^{(i)}$ such that:

$$\kappa \geq \max_{\substack{(\mathbf{x},\mathbf{q}) \in \mathcal{G} \\ \mathbf{p} \in \overline{B}_{\overline{\Delta}}}} \|\mathbf{f}(\mathbf{x}, \mathbf{q}, \mathbf{p})\| \quad (8)$$

$$\chi \geq \max_{\substack{(\mathbf{x},\mathbf{q}) \in \mathcal{G} \\ \mathbf{p} \in \overline{B}_{\overline{\Delta}}}} \|\mathbf{F}_{\mathbf{x}}(\mathbf{x}, \mathbf{q}, \mathbf{p})^{-1}\| \quad (9)$$

$$\gamma^{(i)} \geq \max_{\substack{(\mathbf{x},\mathbf{q}) \in \mathcal{G} \\ \mathbf{p} \in \overline{B}_{\overline{\Delta}}}} \|\mathbf{F}_{\mathbf{x}}(\mathbf{x}, \mathbf{q}, \mathbf{p})^{-1} \mathbf{F}_{\mathbf{p}^{(i)}}(\mathbf{x}, \mathbf{q}, \mathbf{0})\| \quad (10)$$

where $\mathbf{p}^{(i)}$ form a partition of the perturbation vector $\mathbf{p}$. Define

$$r := 2\kappa\chi, \quad (11)$$

and suppose the two following Lipschitz conditions hold for constants λ and μ

$$\forall (\mathbf{x}_0, \mathbf{q}) \in \mathcal{G}, \forall \mathbf{p} \in \overline{B}_{\overline{\Delta}}, \forall \mathbf{x}', \mathbf{x}'' \in \overline{B}(\mathbf{x}_0, r), \quad \|\mathbf{F}_{\mathbf{x}}(\mathbf{x}', \mathbf{q}, \mathbf{p}) - \mathbf{F}_{\mathbf{x}}(\mathbf{x}'', \mathbf{q}, \mathbf{p})\| \leq \lambda \|\mathbf{x}' - \mathbf{x}''\|, \quad (12)$$

$$\forall (\mathbf{x}, \mathbf{q}) \in \mathcal{G}, \forall \mathbf{p}, \mathbf{p}' \in \overline{B}_{\overline{\Delta}}, \quad \|\mathbf{F}_{\mathbf{p}}(\mathbf{x}, \mathbf{q}, \mathbf{p}) - \mathbf{F}_{\mathbf{p}}(\mathbf{x}, \mathbf{q}, \mathbf{p}')\| \leq \mu \|\mathbf{p} - \mathbf{p}'\|. \quad (13)$$

Theorem 1: Let $\overline{\Delta} > 0$, and $\kappa, \chi, \gamma \geq 0$ be such that (8), (9) and (10) are satisfied. Consider $\lambda, \mu \geq 0$ such that (12) and (13) are satisfied. Define $r := 2\kappa\chi$ as in (11),

$$\eta(\mathbf{p}) := 2 \sum_i \gamma^{(i)} \|\mathbf{p}^{(i)}\| + \mu\chi \|\mathbf{p}\|^2, \quad (14)$$

[1] Fixing the value of $\overline{\Delta}$ can be done with successive adjustments when necessary: Too large or too small values of $\overline{\Delta}$ will result in small perturbation domain.

and the perturbation domain

$$\mathcal{P} = \{\mathbf{p} \in \overline{B}_{\overline{\Delta}} : \lambda\chi\eta(\mathbf{p}) \leq 1\}. \quad (15)$$

Then $\mathcal{G}$ is $\bar{\epsilon}$-safe with respect to $\mathcal{P}$ for

$$\bar{\epsilon} = \min\{r, \frac{1}{\chi\lambda}\}. \quad (16)$$

Furthermore, the distance between the nominal and the perturbed poses is at most

$$\epsilon(\mathbf{p}) := \frac{\eta(\mathbf{p})}{1 + \sqrt{1 - \chi\lambda\eta(\mathbf{p})}}. \quad (17)$$

Proof: Consider an arbitrary nominal pose $(\mathbf{x}_0, \mathbf{q}) \in \mathcal{G}$. We just need to prove that for an arbitrary fixed $\mathbf{p} \in \mathcal{P}$ there exists a unique solution $\mathbf{x}^*$ to $\mathbf{h}(\mathbf{x}) = \mathbf{0}$, with $\mathbf{h}(\mathbf{x}) := \mathbf{f}(\mathbf{x}, \mathbf{q}, \mathbf{p})$, inside $\overline{B}(\mathbf{x}_0, \bar{\epsilon})$, and that this solution satisfies $\|\mathbf{x}_0 - \mathbf{x}^*\| \leq \epsilon(\mathbf{p})$.

To this end, we apply Kantorovich theorem to the resolution of the system $\mathbf{h}(\mathbf{x}) = \mathbf{0}$, starting from the initial condition $\mathbf{x}_0$. Let $D_0 := B(\mathbf{x}_0, r)$. Then by (12), $\mathbf{H}_\mathbf{x}(\mathbf{x}) = \mathbf{F}_x(\mathbf{x}, \mathbf{q}, \mathbf{p})$ is Lipschitz with constant λ inside D_0. By (9), $\mathbf{\Gamma}_0 := \mathbf{H}_\mathbf{x}(\mathbf{x}_0)^{-1}$ is defined and $\|\mathbf{\Gamma}_0\| \leq \chi$. We prove now that

$$\|\mathbf{\Gamma}_0\mathbf{h}(\mathbf{x}_0)\| \leq \frac{1}{2}\min\{r, \eta(\mathbf{p})\} =: \delta. \quad (18)$$

First, $\|\mathbf{\Gamma}_0\mathbf{h}(\mathbf{x}_0)\| \leq \|\mathbf{\Gamma}_0\|\|\mathbf{h}(\mathbf{x}_0)\| \leq \kappa\chi = \frac{r}{2}$, the second inequality resulting of (8) and (9). Second, defining $\mathbf{M} := \mathbf{F}_\mathbf{p}(\mathbf{x}_0, \mathbf{q}, \mathbf{0})$, $\mathbf{M}^{(i)} := \mathbf{F}_{\mathbf{p}^{(i)}}(\mathbf{x}_0, \mathbf{q}, \mathbf{0})$ and $\mathbf{z} := \mathbf{h}(\mathbf{x}_0) - \mathbf{M}\mathbf{p}$,

$$\begin{aligned}
\|\mathbf{\Gamma}_0\mathbf{h}(\mathbf{x}_0)\| &= \|\mathbf{\Gamma}_0(\mathbf{M}\mathbf{p} + \mathbf{z})\| & (19)\\
&= \|\mathbf{\Gamma}_0\Big(\sum_i \mathbf{M}^{(i)}\mathbf{p}^{(i)} + \mathbf{z}\Big)\| & (20)\\
&\leq \sum_i \|\mathbf{\Gamma}_0\mathbf{M}^{(i)}\|\|\mathbf{p}^{(i)}\| + \|\mathbf{\Gamma}_0\|\|\mathbf{z}\| & (21)\\
&\leq \sum_i \gamma^{(i)}\|\mathbf{p}^{(i)}\| + \chi\|\mathbf{z}\|, & (22)
\end{aligned}$$

where the last inequality follows from (9) and (10). Finally, following the classical argument given in [15], [8], and using (13), we have $\|\mathbf{z}\| \leq \frac{1}{2}\mu\|\mathbf{p}\|^2$, which proves (18).

Now, it remains to prove that $h := 2\chi\lambda\delta \leq 1$ and that $B(\mathbf{x}_0, t^*) \subseteq D_0$, where $t^* := \frac{2\delta(1-\sqrt{1-h})}{h}$. First,

$$h = 2\chi\lambda\delta \underset{(18)}{\leq} \lambda\chi\eta(\mathbf{p}) \underset{(15)}{\leq} 1, \quad (23)$$

Second, we have

$$t^* \underset{(57)}{\leq} 2\delta \underset{(18)}{\leq} r. \quad (24)$$

Therefore, $B(\mathbf{x}_0, t^*) \subseteq B(\mathbf{x}_0, r) = D_0$.

Therefore we can apply Kantorovich theorem [10] which proves that $\mathbf{h}(\mathbf{x})$ has a solution $\mathbf{x}^*$ inside $\overline{B}(\mathbf{x}_0, t^*)$ with $\mathbf{H}_\mathbf{x}(\mathbf{x}^*)$ nonsingular, and that this solution is unique inside $\overline{B}(\mathbf{x}_0, \bar{\epsilon}) \supseteq \overline{B}(\mathbf{x}_0, t^*)$: On the one hand, if $h \in [0, 1)$ then Kantorovich theorem proves that it is unique inside $B(\mathbf{x}_0, t') \cap D_0$, while

$$B(\mathbf{x}_0, t') \cap D_0 \underset{(56)}{\supseteq} \overline{B}(\mathbf{x}_0, \frac{1}{\chi\lambda}) \cap D_0 \underset{(16)}{=} \overline{B}(\mathbf{x}_0, \bar{\epsilon}). \quad (25)$$

On the other hand, if $h = 1$ then Kantorovich theorem proves that it is unique inside $\overline{B}(\mathbf{x}_0, t')$, while

$$\overline{B}(\mathbf{x}_0, t') \underset{(55)}{=} \overline{B}(\mathbf{x}_0, \frac{1}{\chi\lambda}) \underset{(16)}{\supseteq} \overline{B}(\mathbf{x}_0, \bar{\epsilon}). \quad (26)$$

Finally, using $2\delta \leq \eta(\mathbf{p})$, which holds by (18), we have $h = 2\chi\lambda\delta \leq \chi\lambda\eta(\mathbf{p})$, and eventually

$$t^* = \frac{2\delta}{1 + \sqrt{1 - h}} \leq \epsilon(\mathbf{p}), \quad (27)$$

therefore $\|\mathbf{x}_0 - \mathbf{x}^*\| \leq \epsilon(\mathbf{p})$. ■

Remark 2: The perturbation domain $\mathcal{P}$ provided by Theorem 1 is convex. Indeed, it has the form $\mathbf{a}^T\mathbf{p} + b\|\mathbf{p}\|^2 \leq 1$, with $b > 0$, so $\mathbf{a}^T\mathbf{p} + b\|\mathbf{p}\|^2$ is the sum of two convex functions.

Remark 3: Kantorovich Theorem also proves

$$\forall(\mathbf{x}, \mathbf{q}) \in \mathcal{G}, \forall\mathbf{p} \in \mathcal{P}, \forall\mathbf{x}' \in \overline{B}(\mathbf{x}, \bar{\epsilon}), \det \mathbf{F}_\mathbf{x}(\mathbf{x}', \mathbf{q}, \mathbf{p}) \neq 0, \quad (28)$$

which is of great practical interest, since for the perturbation domain considered, it proves that no perturbed pose leads to any parallel singularity.

B.3 Asymptotic analysis

It can be seen from the definition (14) that $\eta(\mathbf{p}) \approx 2\sum_i \gamma^{(i)}\|\mathbf{p}^{(i)}\|$ provided that

$$\|\mathbf{p}\|^2 \ll \frac{2}{\mu\chi}\sum_i \gamma^{(i)}\|\mathbf{p}^{(i)}\|, \quad (29)$$

which is satisfied as soon as $\|\mathbf{p}\|$ is small enough. If furthermore $\chi\lambda\eta(\mathbf{p}) \approx 2\chi\lambda\sum_i \gamma^{(i)}\|\mathbf{p}^{(i)}\|$ is small with respect to 1 then $\epsilon(\mathbf{p}) \approx \frac{\eta(\mathbf{p})}{2} = \sum_i \gamma^{(i)}\|\mathbf{p}^{(i)}\|$. Figure 1 shows the typical behavior of $\eta(\mathbf{p})$, $\epsilon(\mathbf{p})$, $\bar{\epsilon}$ and $\gamma_0\|\mathbf{p}\|$ in the case where $\mathbf{p}$ is not split (i.e., $\sum_i \gamma^{(i)}\|\mathbf{p}^{(i)}\| = \gamma\|\mathbf{p}\|$).

Another interesting observation is that, under the validity of the approximation $\eta(\mathbf{p}) \approx 2\sum_i \gamma^{(i)}\|\mathbf{p}^{(i)}\|$, the size of the perturbation domain $\{\mathbf{p} \in \overline{B}_{\overline{\Delta}} : \lambda\chi\eta(\mathbf{p}) \leq 1\}$ is proportional to the inverse of χ, λ and $\gamma^{(i)}$.

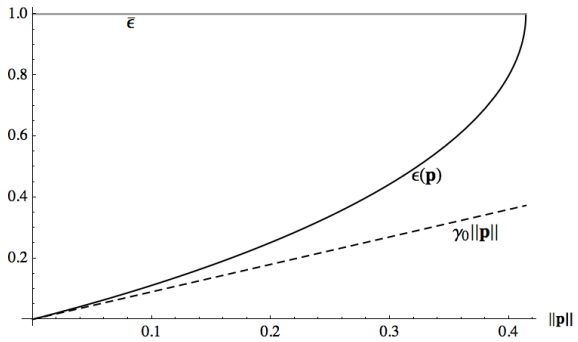

Fig. 1. Typical upper bounds provided by Theorem 1, obtained with the dummy constants $\kappa = \chi = \gamma = \lambda = \mu = 1$ and $\gamma_0 = 0.9$.

IV. Tolerance synthesis

Let $\mathcal{P}$ be the perturbation domain provided by Theorem 1. Our aim is to determine a vector of tolerances $\boldsymbol{\Delta} = (\Delta_i)$ such that

$$\mathcal{S}_{\boldsymbol{\Delta}} := \{\mathbf{p} \in \mathbb{R}^m : \|\mathbf{p}^{(i)}\| \leq \Delta_i\} \tag{30}$$

is contained inside $\mathcal{P}$, and that the error $e(\mathbf{x}, \mathbf{x}')$ is less than a given threshold $\bar{e}$ for all perturbations in $\mathcal{S}_{\boldsymbol{\Delta}}$.

In Subsection IV-A, we propose a non-rigorous linear approximation of the maximal error in the workspace. In Subsection IV-B, we formulate the Tolerance synthesis as a multi-objective optimization problem, aiming maximizing the different tolerances Δ_i. Finally, a certified upper bound for the pose error corresponding to the tolerances synthesized by this process is computed by solving the optimization problem described Section III.

A. Approximate linearization of the pose error

Theorem 1 involves several overestimations, which leads to an overestimated error upper bound for the considered perturbation domain. This allows making the assumption that a linear approximation is going to be accurate within the perturbation domain provided by Theorem 1. Therefore, we make the assumption that the following linear approximation holds:

$$\mathbf{x}' - \mathbf{x} \approx \mathbf{F}_{\mathbf{x}}(\mathbf{x}, \mathbf{q}, \mathbf{0})^{-1} \mathbf{F}_{\mathbf{p}}(\mathbf{x}, \mathbf{q}, \mathbf{0}) \mathbf{p}. \tag{31}$$

We obtain an approximate workspace worst case error $e(\mathbf{x}, \mathbf{x}') = \|\boldsymbol{\Pi}(\mathbf{x} - \mathbf{x}')\|$ in the following way: Using (31), we obtain that (7) is approximately

$$\max_{\substack{(\mathbf{x},\mathbf{q}) \in \mathcal{G} \\ \mathbf{p} \in \mathcal{S}_{\boldsymbol{\Delta}}}} \|\boldsymbol{\Pi} \mathbf{F}_{\mathbf{x}}(\mathbf{x}, \mathbf{q}, \mathbf{0})^{-1} \mathbf{F}_{\mathbf{p}}(\mathbf{x}, \mathbf{q}, \mathbf{0}) \mathbf{p}\|, \tag{32}$$

which we approximate by

$$\max_{\substack{(\mathbf{x},\mathbf{q}) \in \mathcal{G} \\ \mathbf{p} \in \mathcal{S}_{\boldsymbol{\Delta}}}} \|\boldsymbol{\Pi} \mathbf{F}_{\mathbf{x}}(\mathbf{x}, \mathbf{q}, \mathbf{0})^{-1} \mathbf{F}_{\mathbf{p}}(\mathbf{x}, \mathbf{q}, \mathbf{0})\| \|\mathbf{p}\|. \tag{33}$$

We finally approximate (33) by

$$\max_{\mathbf{p} \in \mathcal{S}_{\boldsymbol{\Delta}}} \sum_i \gamma_0^{(i)} \|\mathbf{p}^{(i)}\| = \sum_i \gamma_0^{(i)} \Delta_i, \tag{34}$$

where

$$\gamma_0^{(i)} = \max_{(\mathbf{x},\mathbf{q}) \in \mathcal{G}} \|\boldsymbol{\Pi} \mathbf{F}_{\mathbf{x}}(\mathbf{x}, \mathbf{q}, \mathbf{0})^{-1} \mathbf{F}_{\mathbf{p}^{(i)}}(\mathbf{x}, \mathbf{q}, \mathbf{0})\|. \tag{35}$$

Although it is difficult to assess the accuracy of this linear approximation in general, it turns out to be very accurate in the preliminary experiments presented in Section V.

B. Approximate tolerance synthesis and its validation

In order to be able to compute a rigorous pose error upper bound using Theorem (1), we need to choose Δ_i using (34) under the additional constraint that $\mathcal{S}_{\boldsymbol{\Delta}}$ is a subset of $\mathcal{P}$. Therefore, admissible tolerances $\boldsymbol{\Delta}$ satisfy

$$\sum_i \gamma_0^{(i)} \Delta_i \leq \bar{e} \tag{36}$$

$$2 \sum_i \gamma^{(i)} \Delta_i + \mu\chi \|\boldsymbol{\Delta}\|^2 \leq \frac{1}{\lambda\chi} \tag{37}$$

$$\|\boldsymbol{\Delta}\| \leq \overline{\Delta}, \tag{38}$$

where (37) and (38) encode $\mathcal{S}_{\boldsymbol{\Delta}} \subseteq \mathcal{P}$ (the constraint (37) comes from (14) and (15), while (38) is the a priori maximal perturbation norm). As mentioned earlier, the domain (37) is convex, and so is the set of admissible tolerances defined by (36), (37) and (38). Finally, we want to select tolerances satisfying (36), (37) and (38) that maximizes each Δ_i in a multi-objective sense, i.e., that are Pareto optimal for these objectives. Since objectives and constraints are convex and almost linear, this multi-objective optimization problem is actually trivial to solve.

Then, solving the optimization problem (7) provides a rigorous upper bound for the pose error over the workspace for the synthesized tolerances. Two cases arise: Either the rigorous upper bound (7) is close enough to the approximate one (34) so that the synthesized tolerances can be used, or the process can be repeated for neighbor tolerances in order to achieve better tolerances. In the experiments presented in the next section, the approximate upper bound (34) is very accurate, but this will have to be investigated on more models.

V. Preliminary experiments

In this section, we provide some first simulations to assess the usefulness of the proposed method. The upper bounds κ, χ, $\gamma^{(i)}$ and $\gamma_0^{(i)}$ have been rigorously computed solving the optimization problems (8), (9), (10) and (35) using the global solver IBEX[2] [7], [17], [1]. It allows comput-

[2]Optimization problems to be solved are non-convex, non-smooth and equality and inequality constrained, and we require rigorous upper bounds. Up to our knowledge, IBEX is the only software available that is able to solve such problems. It can be downloaded from `http://www.ibex-lib.org/`.

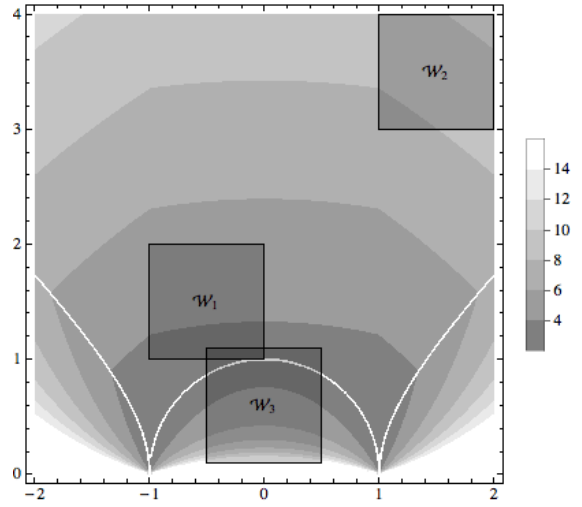

Fig. 2. Sensitivity index and the three workspaces considered for the RPRPR robot (white curves are drawing artefacts due to the non-differentiability of the sensitivity index).

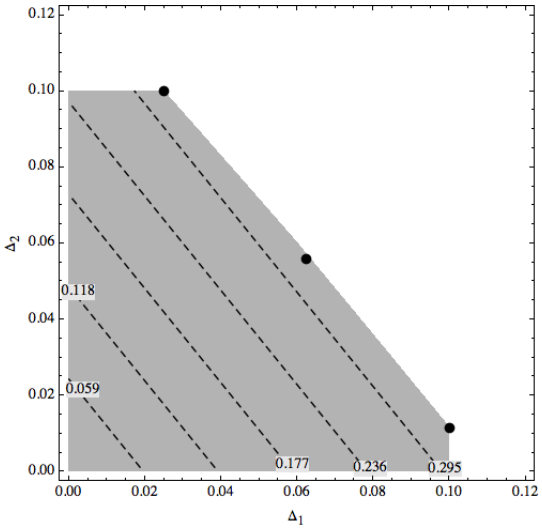

Fig. 3. In gray, the perturbation domain given by Theorem 1 for $\mathcal{W}_1$ (note that it is truncated by $\|\mathbf{\Delta}\| \leq \overline{\Delta}$). Dashed lines represent the error isocontours obtained with the linearization approximation (34).

ing an arbitrarily sharp certified upper bound of these optimization problems, and we stopped the computations when the relative precision of the maximum is 1% (all presented upper bounds are therefore certified and accurate). All computations have been performed on an Intel i7 2.80GHz, the code has not been parallelized, and all timing are given in seconds (a 1 hour timeout has been enforced).

Two different robots are investigated: A RPRPR in Subsection V-A and a 3RPR, with constant orientation, in Subsection V-B. We consider no joint limits, i.e. $q_i \in [0, +\infty)$. The generalized workspace of interest is defined by a rectangular domain in the cartesian space: $\mathbf{x} \in [\underline{\mathbf{x}}, \overline{\mathbf{x}}] =: \mathcal{W}$. Therefore,

$$\mathcal{G} = \{(\mathbf{x}, \mathbf{q}) \in \mathbb{R}^{2n} : \mathbf{f}(\mathbf{x}, \mathbf{q}) = \mathbf{0}, \underline{\mathbf{x}} \leq \mathbf{x} \leq \overline{\mathbf{x}}\}. \quad (39)$$

Several workspaces $\mathcal{W}_i$ are going to be investigated for each robot.

Remark 4: We formally inverse the matrix $\mathbf{F}_{\mathbf{x}}(\mathbf{x}, \mathbf{q}, \mathbf{p})$ in order to solve (9) and (10). Tackling higher dimensional problems will require investigating some rigorous numerical inverse enclosure methods.

A. The RPRPR robot

In this subsection, we study the simple parallel robot RPRPR with 6 perturbations, 4 of them acting on the anchor points, and 2 of them on the commands. Its kinematic model $\mathbf{F}(\mathbf{x}, \mathbf{q}, \mathbf{p})$ is therefore

$$(1 + p_1 + x_1)^2 + (p_2 + x_2)^2 - (p_3 - q_1)^2 \quad (40)$$
$$(-1 + p_4 + x_1)^2 + (p_5 + x_2)^2 - (p_6 - q_2)^2. \quad (41)$$

Since there is not orientation error, we use $e(\mathbf{x}, \mathbf{x}') = \|\mathbf{x} - \mathbf{x}'\|$, i.e. $\mathbf{\Pi}$ is the identity matrix. Perturbations are partitioned in two classes: The geometric perturbations $\mathbf{p}^{(1)} = (p_1, p_2, p_4, p_5)$ and command perturbations $\mathbf{p}^{(2)} = (p_3, p_6)$. The three different workspaces to be investigated are displayed on Figure 2. This figure also shows the level-sets of the sensitivity index

$$\|\mathbf{F}_{\mathbf{x}}(\mathbf{x}, \mathbf{q}(\mathbf{x}), \mathbf{0})^{-1} \mathbf{F}_{\mathbf{p}}(\mathbf{x}, \mathbf{q}(\mathbf{x}), \mathbf{0})\|, \quad (42)$$

where $\mathbf{q}(\mathbf{x})$ is the inverse kinematic model. We expect from Figure 2 that $\mathcal{W}_1$ is the best in term of sensitivity and tolerance synthesis.

The kinematic model involves only quadratic constraints, for which we can easily obtain tight Lipschitz constants for the derivatives: $\lambda = 2$ and $\mu = 2$.

A.1 Workspace $\mathcal{W}_1$

The first workspace we consider is defined by $-1 \leq x_1 \leq 0$ and $1 \leq x_2 \leq 2$. The constants upper bounds computed for this workspace using $\overline{\Delta} = 0.1$ are given in the following table, as well as the time needed to compute them:

	κ	χ	$\gamma^{(1)}$ ($\gamma_0^{(1)}$)	$\gamma^{(2)}$ ($\gamma_0^{(2)}$)
u.b.	1.39	0.64	3.5 (3.01)	2.97 (2.43)
t.	2.6	5.1	0.5 (0.1)	0.2 (0.1)

The corresponding error upper bound given by Theorem 1 is $\overline{\epsilon} = 0.79$. The perturbation domain given by Theorem 1 is shown on Figure 3, as well as the isocontours of the linearized error

$$e(\Delta_1, \Delta_2) \approx 3.01\Delta_1 + 2.43\Delta_2. \quad (43)$$

The three points represent three different compromises of tolerance design, which maximize the tolerances inside

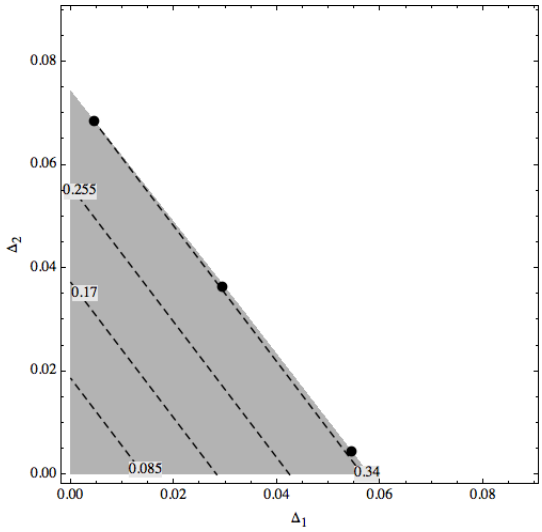

Fig. 4. In gray, the perturbation domain given by Theorem 1 for $\mathcal{W}_2$. Dashed lines represent the error isocontours obtained with the linearization approximation (34).

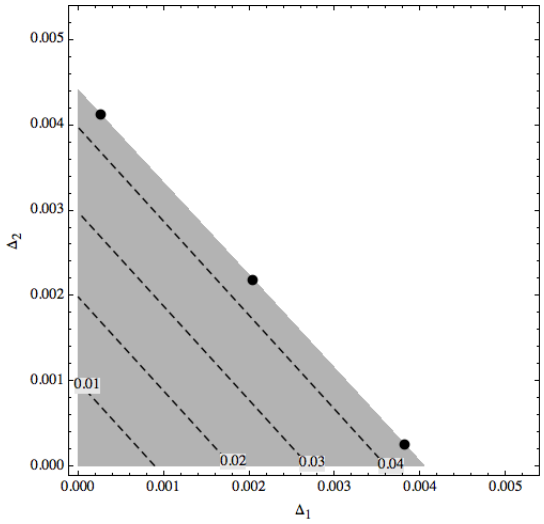

Fig. 5. In gray, the perturbation domain given by Theorem 1 for $\mathcal{W}_3$. Dashed lines represent the error isocontours obtained with the linearization approximation (34).

the perturbation domain provided by Theorem 1. The following table shows for each of them the linearized error, the error upper bound obtained solving (7) using IBEX, as well as the solving time.

Δ	linearized	certified	time
(0.101,0.012)	0.33	0.33	1.11
(0.025,0.101)	0.32	0.31	1.23
(0.063,0.056)	0.33	0.32	0.79

We see that the linearized error is accurate inside the perturbation domain provided by Theorem 1. The tolerance synthesis can therefore be performed inside this perturbation domain using the linearized errors by solving the bi-objective problem consisting of maximizing Δ_1 and Δ_2 subject to (36), (37) and (38), and eventually checking the chosen tolerances a posteriori solving (7).

A.2 Workspace $\mathcal{W}_2$

The first workspace we consider is defined by $1 \leq x_1 \leq 2$ and $3 \leq x_2 \leq 4$. The constants upper bounds computed for this workspace using $\overline{\Delta} = 0.1$ are given in the following table, as well as the time needed to compute them:

	κ	χ	$\gamma^{(1)}$ ($\gamma_0^{(1)}$)	$\gamma^{(2)}$ ($\gamma_0^{(2)}$)
u.b.	2.44	0.61	7.05 (6.01)	5.48 (4.57)
t.	0.8	0.1	0.1 (0.1)	0.1 (0.1)

The corresponding error upper bound given by Theorem 1 is $\bar{\epsilon} = 0.83$. The perturbation domain given by Theorem 1 is shown on Figure 4, as well as the isocontours of the linearized error

$$e(\Delta_1, \Delta_2) \approx 6.01\Delta_1 + 4.57\Delta_2. \qquad (44)$$

The three points represent three different compromises of tolerance design, which maximize the tolerances inside the perturbation domain provided by Theorem 1. The following table shows for each of them the linearized error, the error upper bound obtained solving (7) using IBEX, as well as the solving time.

Δ	linearized	certified	time
(0.055,0.005)	0.35	0.35	1.13
(0.005,0.069)	0.34	0.34	1.71
(0.03,0.037)	0.35	0.34	1.34

We see that the linearized error is accurate inside the perturbation domain provided by Theorem 1. The tolerance synthesis can therefore be performed inside this perturbation domain using the linearized errors by solving the bi-objective problem consisting of maximizing Δ_1 and Δ_2 subject to (36), (37) and (38), and eventually checking the chosen tolerances a posteriori solving (7).

When compared with $\mathcal{W}_1$, we see that the linearized error is approximately twice bigger, while the perturbation domain provided by Theorem 1 is twice smaller. The workspace $\mathcal{W}_1$ is therefore better with respect to sensitivity and tolerance synthesis.

A.3 Workspace $\mathcal{W}_3$

The first workspace we consider is defined by $-0.5 \leq x_1 \leq 0.5$ and $0.1 \leq x_2 \leq 1.1$. The constants upper bounds computed for this workspace using $\overline{\Delta} = 0.005$[3] are given in the following table, as well as the time needed to compute them:

[3]This workspace is closer to parallel singularities, and sensibly larger $\overline{\Delta}$ leads to perturbed poses with parallel singularities.

	κ	χ	$\gamma^{(1)}$ ($\gamma_0^{(1)}$)	$\gamma^{(2)}$ ($\gamma_0^{(2)}$)
u.b.	0.05	5.28	11.66 (11.09)	10.72 (10.07)
t.	115.8	0.1	0.1 (0.1)	0.1 (0.1)

The corresponding error upper bound given by Theorem 1 is $\bar{\epsilon} = 0.1$. The perturbation domain given by Theorem 1 is shown on Figure 5, as well as the linearized error $e(\Delta_1, \Delta_2) \approx 11.09\Delta_1 + 10.07\Delta_2$ isocontours.

The three points represent three different compromises of tolerance design, which maximize the tolerances inside the perturbation domain provided by Theorem 1. The following table shows for each of them the linearized error, the error upper bound obtained solving (7) using IBEX, as well as the solving time.

$\boldsymbol{\Delta}$	linearized	certified	time
(0.004,0.001)	0.05	0.04	6.55
(0.001,0.005)	0.05	0.04	4.37
(0.003,0.003)	0.05	0.04	6.81

We see that the linearized error is accurate inside the perturbation domain provided by Theorem 1. The tolerance synthesis can therefore be performed inside this perturbation domain using the linearized errors by solving the bi-objective problem consisting of maximizing Δ_1 and Δ_2 subject to (36), (37) and (38), and eventually checking the chosen tolerances a posteriori solving (7).

When compared with $\mathcal{W}_1$, we see that the linearized error is now approximately 4 times bigger, while the perturbation domain provided by Theorem 1 is now 20 times smaller. The workspace $\mathcal{W}_3$ is therefore the worst with respect to sensitivity and tolerance synthesis.

B. The 3RPR robot

We now study the parallel robot 3RPR with 9 perturbations, 6 of them acting on the anchor points, and 3 of them on the commands. Its kinematic model $\mathbf{F}(\mathbf{x}, \mathbf{q}, \mathbf{p})$ is

$$(d_1 - x_1)^2 + (d_2 - x_2)^2 - (d_3 + q_1)^2 \tag{45}$$

$$\left(L+d_4-x_1-l\sin(\frac{\pi}{6}+x_3)\right)^2+\left(d_5-x_2+l\cos(\frac{\pi}{6}+x_3)\right)^2 - (d_6 + q_2)^2 \tag{46}$$

$$\left(\frac{L}{2}+d_7-x_1-l\cos(x_3)\right)^2+\left(\frac{L\sqrt{3}}{2}+d_8-x_2-l\sin(x_3)\right)^2 - (d_9 + q_3)^2, \tag{47}$$

with $L = 1$ and $l = 0.5$. We study both the position error $e_{\mathrm{P}}(\mathbf{x}, \mathbf{x}') = \|\mathbf{\Pi}_{\mathrm{P}}(\mathbf{x}-\mathbf{x}')\| = \max\{|x_1-x_1'|, |x_2-x_2'|\}$ and the orientation error $e_{\mathrm{O}}(\mathbf{x}, \mathbf{x}') = \|\mathbf{\Pi}_{\mathrm{O}}(\mathbf{x}-\mathbf{x}')\| = |x_3-x_3'|$. Perturbations are partitioned in two classes: The geometric perturbations $\mathbf{p}^{(1)} = (p_1, p_2, p_4, p_5, p_7, p_8)$ and command perturbations $\mathbf{p}^{(2)} = (p_3, p_6, p_9)$. The two different

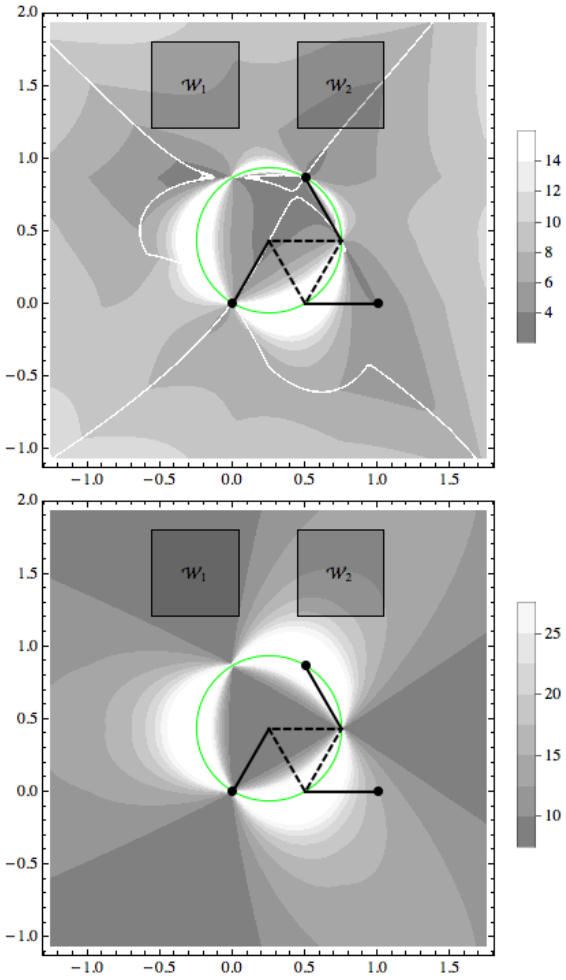

Fig. 6. Sensitivity indices and the two workspaces considered for the 3RPR robot (the green circle represents parallel singularities; the white curves are drawing artefacts due to the non-differentiability of the sensitivity index). The upper graphic and the lower graphics correspond to position and orientation sensitivities respectively.

workspaces to be investigated are displayed on Figure 2, where only x_1 and x_2 are represented because the orientation is fixed to $x_3 = 0$ for each considered workspace. This figure also shows the level-sets of the sensitivity index

$$\|\mathbf{\Pi}\mathbf{F}_{\mathbf{x}}(\mathbf{x}, \mathbf{q}(\mathbf{x}), \mathbf{0})^{-1}\mathbf{F}_{\mathbf{p}}(\mathbf{x}, \mathbf{q}(\mathbf{x}), \mathbf{0})\|, \tag{48}$$

where $\mathbf{q}(\mathbf{x})$ is the inverse kinematic model, $\mathbf{\Pi} = \mathbf{\Pi}_{\mathrm{P}}$ for the upper graphic, and $\mathbf{\Pi} = \mathbf{\Pi}_{\mathrm{O}}$ for the lower graphic. We expect from Figure 2 that $\mathcal{W}_1$ is the best in term of sensitivity and tolerance synthesis.

The kinematic model is not quadratic anymore with respect to $\mathbf{x}$, therefore we solve the following optimization problem, whose upper bound provides a second derivatives based Lipschitz constant satisfying (12):

$$\lambda \geq \max_{\substack{(\mathbf{x},\mathbf{q})\in\mathcal{G} \\ \mathbf{p}\in\overline{B}_{\Delta}}} \max_i \sum_{jk} \left|\frac{\partial f_i}{\partial x_j x_k}(\mathbf{x}, \mathbf{q}, \mathbf{p})\right|. \tag{49}$$

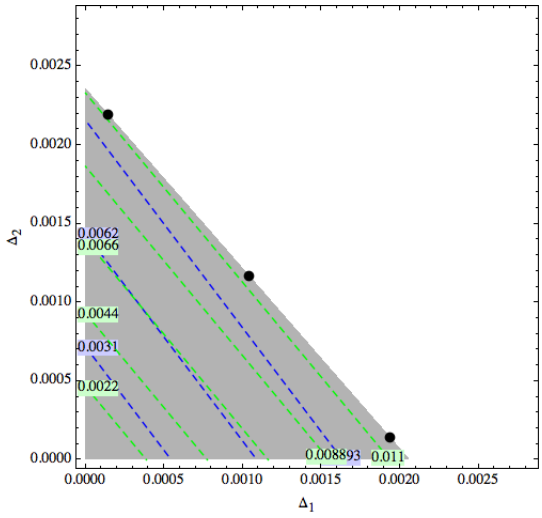

Fig. 7. In gray, the perturbation domain given by Theorem 1 for $\mathcal{W}_1$. Dashed lines represent the error isocontours obtained with the linearization approximation (34).

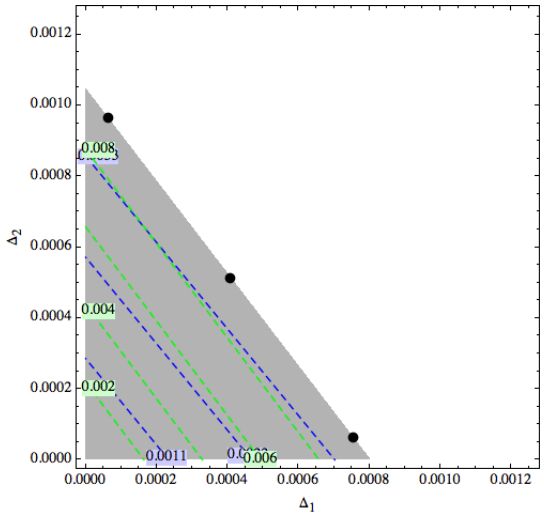

Fig. 8. In gray, the perturbation domain given by Theorem 1 for $\mathcal{W}_2$. Dashed lines represent the error isocontours obtained with the linearization approximation (34).

The kinematic model is quadratic with respect to $\mathbf{p}$, and we can obtain the sharp Lipschitz constant $\mu = 2$.

IBEX resolution timings are quite higher than for the RPRPR robot, because more variables are involved and expressions are more complex. On the other hand, the standard version of IBEX has been used, and specific tuning may turn out to significantly reduce the resolution timings.

B.1 Workspace $\mathcal{W}_1$

The first workspace we consider is defined by $-0.55 \leq x_1 \leq 0.05$, $1.2 \leq x_2 \leq 1.8$ and $x_3 = 0$. The constants upper bounds computed for this workspace using $\overline{\Delta} = 0.01$ are given in the following table, as well as the time needed to compute them:

	κ	χ	λ	$\gamma^{(1)}$ ($\gamma_0^{(1)}$)	$\gamma^{(2)}$ ($\gamma_0^{(2)}$)
u.b. (pos.)	0.1	4.49	9.08	5.95 (5.69)	5.2 (4.31)
u.b. (ori.)				(5.68)	(4.72)
t. (pos.)	9.7	1.1	0.1	49.4 (0.7)	4.8 (0.5)
t. (ori.)				(1.7)	(1.7)

The corresponding error upper bound given by Theorem 1 is $\overline{\epsilon} = 0.03$. The perturbation domain given by Theorem 1 is shown on Figure 7, as well as the isocontours of the linearized position (blue dashed lines) and orientation (green dashed lines) errors

$$e_{\mathrm{P}}(\Delta_1, \Delta_2) \approx 5.69\Delta_1 + 4.31\Delta_2 \quad (50)$$

$$e_{\mathrm{O}}(\Delta_1, \Delta_2) \approx 5.68\Delta_1 + 4.72\Delta_2. \quad (51)$$

The three points represent three different compromises of tolerance design, which maximize the tolerances inside the perturbation domain provided by Theorem 1. The following table shows for each of them the linearized error, the error upper bound obtained solving (7) using IBEX, as well as the solving time.

$100\boldsymbol{\Delta}$	linearized	certified	time
(2,1)	0.012	0.013	606.7
	0.012	0.012	657.4
(1,3)	0.011	0.011	579.9
	0.012	0.012	92.7
(2,2)	0.011	0.012	621.7
	0.012	0.012	47.1

We see that the linearized error is accurate inside the perturbation domain provided by Theorem 1. The tolerance synthesis can therefore be performed inside this perturbation domain using the linearized errors by solving the bi-objective problem consisting of maximizing Δ_1 and Δ_2 subject to (36), (37) and (38), and eventually checking the chosen tolerances a posteriori solving (7).

B.2 Workspace $\mathcal{W}_2$

The first workspace we consider is defined by $0.45 \leq x_1 \leq 1.05$, $1.2 \leq x_2 \leq 1.8$ and $x_3 = 0$. The constants upper bounds computed for this workspace using $\overline{\Delta} = 0.01$ are given in the following table, as well as the time needed to compute them:

	κ	χ	λ	$\gamma^{(1)}$ ($\gamma_0^{(1)}$)	$\gamma^{(2)}$ ($\gamma_0^{(2)}$)
u.b. (pos.)	0.11	5.73	8.58	12.7 (4.7)	9.8 (3.8)
u.b. (ori.)				(12.1)	(9.1)
t. (pos.)	6.6	0.9	0.2	3.1 (0.7)	6.7 (0.8)
t. (ori.)				(0.6)	(0.9)

The corresponding error upper bound given by Theo-

rem 1 is $\bar{\epsilon} = 0.03$. The perturbation domain given by Theorem 1 is shown on Figure 8, as well as the isocontours of the linearized position (blue dashed lines) and orientation (green dashed lines) errors

$$e_{\mathrm{P}}(\Delta_1, \Delta_2) \approx 4.7\Delta_1 + 3.85\Delta_2 \quad (52)$$

$$e_{\mathrm{O}}(\Delta_1, \Delta_2) \approx 12.16\Delta_1 + 9.13\Delta_2. \quad (53)$$

The three points represent three different compromises of tolerance design, which maximize the tolerances inside the perturbation domain provided by Theorem 1. The following table shows for each of them the linearized error, the error upper bound obtained solving (7) using IBEX, as well as the solving time.

$1000\boldsymbol{\Delta}$	linearized	certified	time
(0.76,0.07)	0.0038 0.0097	0.0038 0.0098	2333 91
(0.07,0.97)	0.004 0.0096	0.005 0.0097	2112 85
(0.41,0.52)	0.004 0.0097	N.A. 0.0097	T.O. 79

We see that the linearized error is accurate inside the perturbation domain provided by Theorem 1. The tolerance synthesis can therefore be performed inside this perturbation domain using the linearized errors by solving the bi-objective problem consisting of maximizing Δ_1 and Δ_2 subject to (36), (37) and (38), and eventually checking the chosen tolerances a posteriori solving (7).

As predicted by Figure 6, we see that the position linearized error is approximately the same as $\mathcal{W}_1$ (actually slightly better for $\mathcal{W}_2$) but the orientation error is now twice worse. The perturbation domain provided by Theorem 1 is twice smaller as well. The workspace $\mathcal{W}_1$ is therefore better with respect to sensitivity and tolerance synthesis.

References

[1] I. Araya, G. Trombettoni, B. Neveu, and G. Chabert. Upper Bounding in Inner Regions for Global Optimization Under InequalityConstraints. *J. Global Optimization*, 60(2):145–164, 2014.

[2] S. Bai and S. Caro. Design and analysis of a 3-ppr planar robot with u-shape base. In *Proceedings of the 14th International Conference on Advanced Robotics*, Munich, Germany, June 22-26 2009.

[3] N. Berger, R. Soto, A. Goldsztejn, S. Caro, and P. Cardou. Finding the Maximal Pose Error in Robotic Mechanical Systems Using Constraint Programming. In *Proceedings of IEA-AIE 2010*, volume 6096 of *LNAI*, pages 82–91, 2010.

[4] S. Caro, F. Bennis, and P. Wenger. Tolerance synthesis of mechanisms : A robust design approach. *ASME Journal of Mechanical Design*, 127:86–94, January 2005. hal-00463707.

[5] S. Caro, N Binaud, and P. Wenger. Sensitivity Analysis of 3-RPR Planar Parallel Manipulators. *ASME Journal of Mechanical Design*, 131:121005–1–121005–13, 2009.

[6] S. Caro, P. Wenger, F. Bennis, and D. Chablat. Sensitivity analysis of the orthoglide, a 3-dof translational parallel kinematic machine. *ASME Journal of Mechanical Design*, 128:392–402, March 2006.

[7] G. Chabert and L. Jaulin. Contractor Programming. *Artif. Intell.*, 173(11):1079–1100, 2009.

[8] P. G. Ciarlet and C. Mardare. On the Newton-Kantorovich Theorem. *Analysis and Applications*, 10(03):249–269, 2012.

[9] K-C. Fan, H. Wang, J-W. Zhao, and T-H. Chang. Sensitivity analysis of the 3-prs parallel kinematic spindle platform of a serial-parallel machine tool. *International Journal of Machine Tools and Manufacture*, 43:1561–1569, 2003.

[10] W. Gragg and R. Tapia. Optimal Error Bounds for the Newton-Kantorovich Theorem. *SIAM Journal on Numerical Analysis*, 11(1):10–13, 1974.

[11] C. Han, Ji. Kim, Jo. Kim, and Park F.C. Kinematic sensitivity analysis of the 3-upu parallel mechanism. *Mechanism and Machine Theory*, 37:787–798, 2002.

[12] H.S. Kim and Y.J. Choi. The kinematic error bound analysis of the stewart platform. *Journal of Robotic Systems*, 17:63–73, 2000.

[13] H.S. Kim and L-W. Tsai. Design optimization of a cartesian parallel manipulator. *ASME Journal of Mechanical Design*, 125:43–51, 2003.

[14] J.P. Merlet. *Parallel robots*. Kluwer, Dordrecht, 2000.

[15] J. M. Ortega. The Newton-Kantorovich Theorem. *The American Mathematical Monthly*, 75(6):658–660, 1968.

[16] Mikhael Tannous, Stphane Caro, and Alexandre Goldsztejn. Sensitivity analysis of parallel manipulators using an interval linearization method. *Mechanism and Machine Theory*, 71(0):93 – 114, 2014.

[17] Gilles Trombettoni, Ignacio Araya, Bertrand Neveu, and Gilles Chabert. Inner regions and interval linearizations for global optimization. In Wolfram Burgard and Dan Roth, editors, *AAAI*. AAAI Press, 2011.

[18] M. Verner, X. Fengfeng, and C. Mechefske. Optimal calibration of parallel kinematic machines. *ASME Journal of Mechanical Design*, 127:62–69, 2005.

[19] J. Wang and O. Masory. On the accuracy of a stewart platform - part i, the effect of manufacturing tolerances. In *Proceedings of the IEEE International Conference on Robotics Automation, ICRA'93*, 1993.

[20] A. Yu, I. Bonev, and P. Zsombor-Murray. Geometric approach to the accuracy analysis of a class of 3-dof planar parallel robots. *Mechanism and Machine Theory*, 43(3):364–375, 2009.

Appendix

I. Technical results

Lemma 1: With the notations of Kantorovich Theorem [10],

$$t^* = \frac{2\delta(1-\sqrt{1-h})}{h} \text{ and } t' = \frac{2\delta(1+\sqrt{1-h})}{h} \quad (54)$$

we have

$$h = 1 \implies t^* = 2\delta = \frac{1}{\chi\lambda} = t' \quad (55)$$

$$h \in [0,1) \implies t^* < 2\delta < \frac{1}{\chi\lambda} < t' \quad (56)$$

$$h \in [0,1] \implies t^* \leq 2\delta \leq \frac{1}{\chi\lambda} \leq t' \quad (57)$$

Proof: Equation (55) is trivial, and (57) follows from the previous ones. Equation (56) remains to be proved. First note that

$$t^* = \frac{2\delta}{1+\sqrt{1-h}}, \quad (58)$$

which is strictly increasing with respect to h. Therefore, $h \in [0,1)$ implies $t^* < 2\delta$. Second note that

$$t' = \frac{2(1+\sqrt{1-h})}{\chi\lambda}, \quad (59)$$

which is strictly decreasing with respect to h. Therefore, $h \in [0,1)$ implies $\frac{1}{\chi\lambda} < t'$. ■